Numerical Simulation of the HEMP Environment

Cui Meng, *Member, IEEE*

***Abstract*—This paper develops the program MCHII, numerically simulating the physical process of Compton electron currents scattered by the interaction of γ rays with ambient air molecules radiating the early time electromagnetic pulse (E1) during the high altitude nuclear explosion. The paper discusses the waveform characteristics of the electromagnetic pulse E1 as it propagates toward the ground from beneath the explosion point during the high altitude nuclear explosion, and provides a detailed study with regard to the influence of explosion height, energy, and γ spectrum. Numerical simulations are used to present the waveform characteristics of the electromagnetic pulse after going through the ionized layer above the explosion point after the high altitude nuclear explosion, and the paper presents the distribution of high altitude electromagnetic pulse waveform amplitudes at satellite orbits.**

***Index Terms*—Compton scattering, geomagnetic field, HEMP, ionosphere.**

I. Introduction

In publications of IEC SC 77C standards, high-power EM includes the high altitude electromagnetic pulse (HEMP), high-power microwaves, and lightning EMP, etc. [1]. Of these environments, HEMP covers all areas within the visual field of the explosion point and affects the widest scope. With high field intensity and abundant frequency spectra, HEMP couples to electronic systems from front-door and back-door, leading to failure and breakdown of electronic equipment, communication interrupt, and dysfunction of command. It constitutes the difficult and key points in electromagnetic protection and reinforcement. Therefore, it is important to understand the physical properties of the HEMP and to provide standard waveforms of the HEMP environment.

The physical processes involved in a nuclear explosion include nuclear radiation and may also incite strong EMP signals. Such a physical mechanism had been predicted by the physicist Fermi prior to the first nuclear test in U.S. In subsequent high-altitude nuclear explosion tests, HEMP signals were observed. In addition several publications of the past have indicated that it is possible to calculate HEMP at the earth's surface using computer modeling [15], [16]. Consequently, HEMP signals are likely to play an important role of positioning, timing, and compliance identification for nuclear radiation monitoring [2]. When the explosion center is in or below the ionosphere, the lower frequency components of the HEMP signals are obstructed due to the existence of an ionized layer in the air over the earth; the high-frequency portion is chromatically dispersed in the ionized layer. It is therefore necessary to study the feasibility of HEMP monitoring at satellite orbits [3], [4].

II. Physical Mechanism of HEMP Generation

In the IEC 61000-2-9 standard [14], HEMP falls into three types, i.e., early-time, mid-time, and late-time HEMPs, or E1, E2, and E3, respectively. When a nuclear device explodes, the instantaneously emitted γ rays and X rays crash into the ambient gas atoms, knocking out the electrons in the atoms, which fly outward in the radial direction to give rise to "Compton currents." Influenced by atmosphere density, the weapon system, geomagnetism, and the water vapor in the air, the nuclear explosion is not spherically symmetric. Therefore, "Compton currents" will oscillate and radiate a high power electromagnetic pulse, which is called E1. HEMP incited by the interaction of γ rays generated by neutrons in the device radiation with the air is called E2. In addition, the "fireball" generated from the nuclear explosion is a high temperature, high-pressure plasma. The "fireball" excludes the magnetic lines of force of the earth. When the "fireball" expands at a high speed, the magnetic lines of force are compressed; when the "fireball" disappears, the magnetic lines of force return to normal. Such compression and restoration of the magnetic lines of force will arouse electromagnetic radiation inside the earth, which is called E3.

When the point of a nuclear explosion is at high altitude, the instantaneously radiated X rays, γ rays, and neutrons propagate energy under the explosion point. In this area, γ rays act with air molecules to incite Compton electrons. These electrons deflect with the action of geomagnetic field, and the resultant transverse currents draw out transverse electric field when they are transmitted to the Earth's surface. This is the generation mechanism of early-time HEMP known as E1 (see Fig. 1).

III. Physical Model of Calculation

A. Selection of Coordinates

This calculation only included the process of the interaction of Compton electrons incited by γ rays with the geomagnetic field to create the electromagnetic radiation E1. The early-time HEMP incited in this process has the strongest amplitude and abundant frequency spectra.

Fig. 2 shows the geographic structure during the nuclear explosion. In the high altitude nuclear explosion, the γ pulse released from nuclear devices will interact with ambient thin air when it radiates outward, and will scatter Compton-electron currents. Thanks to their huge energy, Compton electrons move forward at a speed close to c, the velocity of light. Due to the very thin air at high altitude, these electrons have a long range. Their movement trail will be violently deflected by the geomagnetic

Manuscript received August 30, 2012; revised March 19, 2013; accepted March 27, 2013. Date of publication May 29, 2013; date of current version June 11, 2013.

The author is with the Key Laboratory of Particle and Radiation Imaging, Ministry of Education, Department of Engineering Physics, Tsinghua University, Beijing 100084, China (e-mail: mengcui@mail.tsinghua.edu.cn).

Color versions of one or more of the figures in this paper are available online at http://ieeexplore.ieee.org.

Digital Object Identifier 10.1109/TEMC.2013.2258024

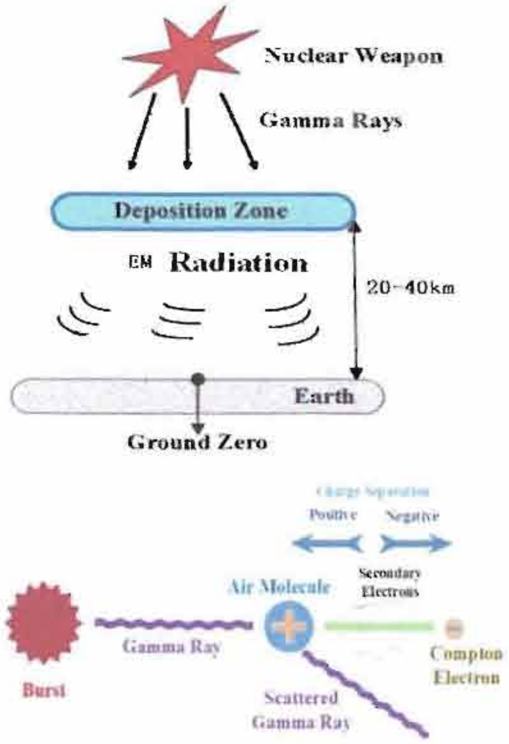

Fig. 1. Generation mechanism of HEMP for the early-time E1.

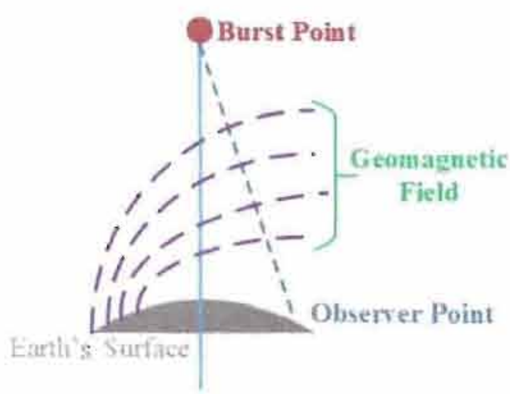

Fig. 2. Geographic location of high altitude nuclear explosion.

field. Thus, Compton currents will have both a radial component J_r and transverse components J_θ and J_ψ in the direction of θ and ψ. If the explosion is axisymmetric to its environment, the radial component J_r and the component J_θ in the direction of θ will incite transverse magnetic waves; the current J_ψ in the direction of ψ will incite transverse electric waves.

The coordinates r, θ, φ are used, with the origin located at the explosion center, and the direction of the polar axis (i.e., axis z for $\theta = 0°$) coinciding with that of geomagnetic field $\vec{B}_0$, i.e., pointing down to the ground (in the Northern Hemisphere). The inclined angle between the geomagnetic field and the vertical axis of ground is supposed to be θ_0. In other words, the magnetic inclination is $\pi/2$–θ_0. In this paper, values $\theta_0 = 30°$ and $\varphi_0 = 0°$ are used in the numerical calculation.

B. Mathematic Equation

The measurement unit of Gauss, cm, g, s, i.e., the static unit for electric charge and electric field was used. The electromagnetic unit was used for electric current and magnetic flux density. Now, the electromagnetic field at any point in the space shall satisfy the Maxwell simultaneous differential equations

$$\frac{1}{c}\frac{\partial \vec{B}}{\partial t} = -\nabla \times \vec{E} \tag{1}$$

$$\frac{\varepsilon\mu}{c}\frac{\partial \vec{E}}{\partial t} + \mu(4\pi\sigma\vec{E} + 4\pi\vec{J}\,) = \nabla \times \vec{B} \tag{2}$$

$$\nabla \cdot (\sigma\vec{E} + \vec{J}\,) + \frac{\partial \rho_f}{\partial t} = 0 \tag{3}$$

$$\nabla \cdot \vec{B} = 0. \tag{4}$$

Considering the electric current J and the secondary electron $n_{\rm sec}$ after the counteraction of the geomagnetic field, the expression is as follows [5]:

$$J_r(r,\theta,\varphi,\tau) \approx -\frac{e_q}{c}\varepsilon g(r)\int_0^{R_e/\beta} d\tau' \dot{f}_\gamma(\tau - \chi(\tau'))$$
$$\times(\cos^2\theta + \sin^2\theta \cdot \cos\omega\tau') \tag{5}$$

$$J_\theta(r,\theta,\varphi,\tau) \approx -\frac{e_q}{c}\varepsilon g(r)\int_0^{R_e/\beta} d\tau' \dot{f}_\gamma(\tau - \chi(\tau'))$$
$$\times \sin\theta \cdot \cos\theta(\cos\omega\tau' - 1) \tag{6}$$

$$J\varphi(r,\theta,\varphi,\tau) \approx -\frac{e_q}{c}\varepsilon g(r)\int_0^{R_e/\beta} d\tau' \dot{f}_\gamma(\tau - \chi(\tau'))$$
$$\times \sin\theta \cdot \sin\omega\tau' \tag{7}$$

$$n_{\rm sec}(r,\theta,\varphi,\tau) \approx \frac{q}{c}\frac{g(r)}{R_e}\int_{-\infty}^{\tau} d\tau' e^{-\alpha(\tau-\tau')}$$
$$\times \int_0^{R_e/\beta} d\tau'' \dot{f}_\gamma(\tau' - \chi(\tau'')) \tag{8}$$

where

$$g(r) = \beta\frac{\exp(-\int_0^r \frac{dr}{\lambda(r,\theta,\varphi)})}{4\pi r^2\lambda(r,\theta,\varphi)},$$

$$\lambda(r,\theta,\varphi) = \frac{\lambda_0\rho_0}{\rho(r,\vartheta,\varphi)},$$

λ_0 is the γ mean free path at the explosion center (cm); ρ_0 is the air density at the center of explosion (mg/cm^3); $\rho(r, \theta, \varphi)$ is the air density of a source point with coordinates (r, θ, φ) (mg/cm^3); $R_e = R_{e0} \cdot \rho_0/\rho(r,\theta,\varphi)$; R_{e0} is the j mean range of a Compton electron or photoelectron at the explosion center (cm); $\beta = v_0/c$, v_0 is the initial speed of a Compton electron or photoelectron (cm/s); $\omega = (e_q \cdot B_0/m_e c^2)\sqrt{1-\beta^2}$ represents the Larmor frequency (cm^{-1}); $e_q = 4.8 \times 10^{-10}$ represents the absolute value of the electric charge of an electron; m_e is the rest mass of the electron; $\alpha = \alpha_0(\rho(r,\theta,\varphi)/\rho_0)^2$; α_0 is the rate of attachment of an electron to an oxygen molecule at the explosion center; $q = (\bar{E}_e/33) \times 10^6$; $\bar{E}_e$ is the average energy of Compton electrons (MeV); and $\dot{f}_\gamma(\tau)$ is the rate of change of γs from the device over time (γ photon/s).

The motion equation of secondary electrons in the electric field is taken into account to find out the expression of conductivity as follows, where v_c represents the collision frequency [6]:

$$\sigma(\tau) = \frac{n_{\mathrm{sec}}(\tau)}{m v_c} e^2. \tag{9}$$

As the range of a γ ray is close to zero at 20 km above the ground, no new electric field will be generated any longer. The outer boundary for the calculation is selected at 20 km above the ground. Then the electric field reaches the ground in the form of plane wave. The electric field near the ground is calculated with the following formula:

$$E = \frac{E_{r\,\max} \cdot r_{\max}}{r_{\mathrm{grd}}}$$

where $r_{\max}$ means the distance of explosion point to the location of 20 km above the ground and r_{grd} means the distance from the explosion point to the ground.

IV. Results of Calculations

A. *Waveform Characteristics and Amplitude Distribution Laws of HEMP on the Ground*

Through calculations we found that, early-time HEMP has the property of a steep rise time and a slightly slower trailing time; the maximum electric field on ground is located in the area of 1–2 explosion heights to the south of the burst point on the ground; the area of minimum electric field is located at 50 km to the north of the burst point on the ground, about one magnitude smaller than the maximum value, as shown in Table I. This depends upon the inclined angle between the motion trail of the Compton electrons in the transmission direction and the geomagnetic field. If the inclined angle is smaller, the incited Compton currents will be smaller, and the field intensity will be smaller; if the inclined angle is bigger, the field intensity will be bigger. For a high altitude explosion at 100 km, the location of 50 km to the north of the projection point of explosion center on the ground is precisely the point of intersection of the geomagnetic line at the explosion center with the ground. The area of 1–2 explosion heights to the south is just the area with an inclined angle of 90° with the geomagnetic line at the explosion center.

Peak electric fields in the west–east directions from the explosion center are symmetrically distributed, with identical waveforms in all fields. This can be explained with a mathematic model. In the west–east direction, φ values are different at symmetrical points, but θ values are identical. In the calculation, φ only appears in the calculation of height. Heights at symmetrical points are identical. Consequently, the results of calculation should be identical. Fields in the direction of E_r cannot radiate outward, so they have a value of zero.

The half width of the time waveform is related to the distance from such point to the projection point of the explosion center on the ground. The smaller this distance (the smaller θ), the narrower the half width of the waveform; HEMP has high

TABLE I
THE ELECTRIC FIELD PEAK VALUE DISTRIBUTED ON THE GROUND FROM A 100 km HOB, 1 MT YIELD BURST

Location on the Ground (Projection Point on the Ground from the Explosion Center)	Peak Electric Field E_ψ (V/m)
50 km to the north	2866
26 km to the north	11447
Ground zero	20777
57.7 km to the south	35494
100 km to the south	40042
173 km to the south	40227
247 km to the south	37071
290 km to the south	34802
514 km to the south	30796

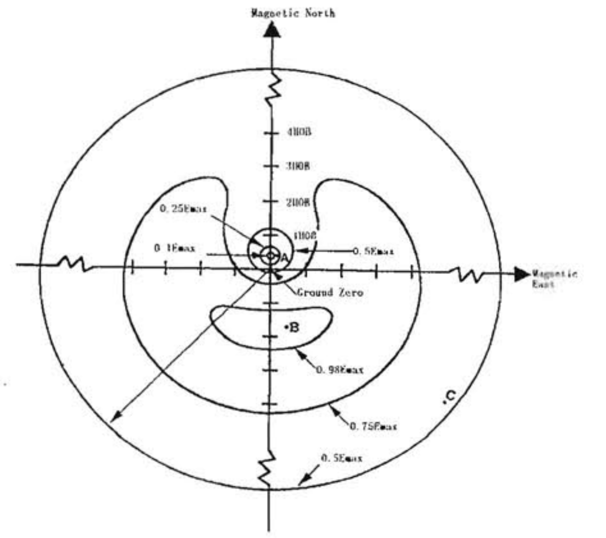

Fig. 3. Typical variations of peak electric fields on the Earth's surface for a high altitude nuclear burst.

electric field amplitudes both in the deposition region and on the ground, ranging from 1 to 100 kV/m (see Table I).

This is consistent with IEC Standard 61000-2-9 published in 1996 [14], as shown in Fig. 3.

On the transmission path from the burst point to the ground, the closer it is to the ground, the narrower the half width of the time waveform. See Fig. 4. The pulsewidth decreases from hundreds of nanoseconds to dozens of nanoseconds. The half width of waveform is generally 20–30 ns near the ground. This is because the closer it comes to the earth's surface, the greater the air density, the greater the value of air conductivity, the faster the low-frequency components at the tail of the waveform decay, and the half width therefore gets smaller.

B. *Influence of the Height of Explosion*

This paper includes the calculation of explosion heights from 100 to 500 km. The field intensity declines slightly as the explosion height rises as shown in Fig. 5. This is consistent with

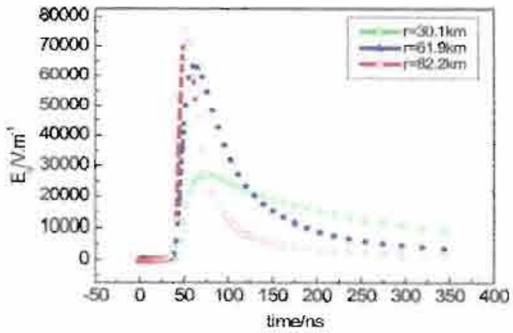

Fig. 4. Waveform of the electric field at different distances from the burst point, $\Psi = 180^0, \theta = 90$.

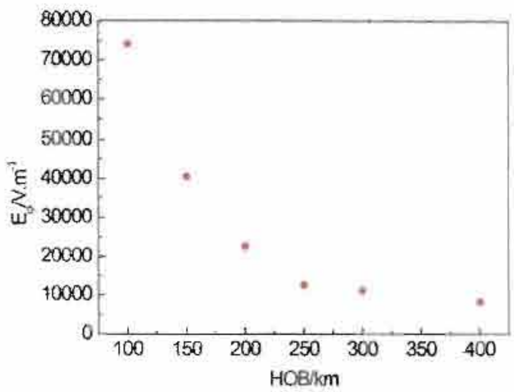

Fig. 5. Relationship between the field strength and HOB (distance from ground zero is 54 km).

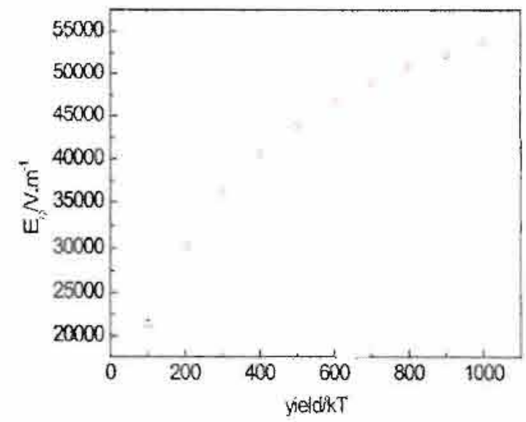

Fig. 6. Distribution of the electric field peak at 110 km from the explosion center with explosion height of 100 km, for different energies, $\theta = 90^\circ$ straight South of the explosion point.

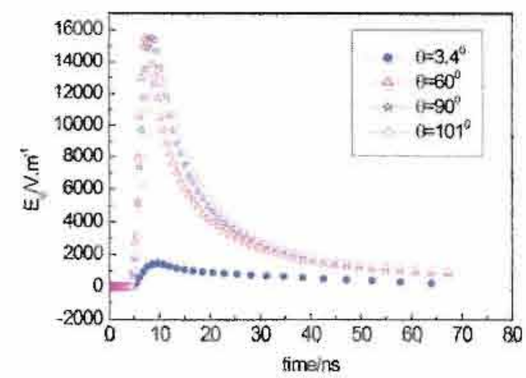

Fig. 7. Calculation result for a 2 ns leading edge of γ rays.

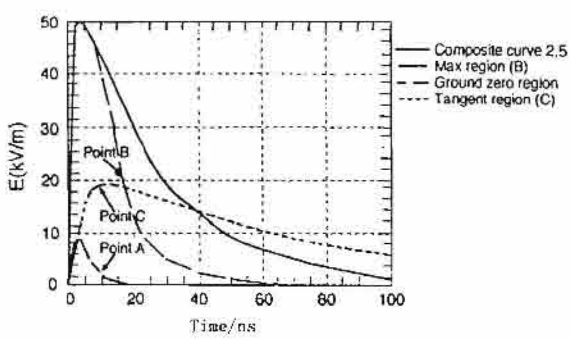

Fig. 8. Recommended waveform in IEC 61000-2-9 [14].

the calculation result in the literature [9]. The energy of γ rays from the explosion decays along the radial direction at the rate of $1/4\pi r^2$. The greater the height of explosion, the greater the distance to the energy deposition area, the greater the attenuation, and the lower the energy of γ rays deposited, thus the weaker the induced EMP.

C. *Influence of the Explosion Energy*

The electric field peak rises as the explosion energy increases. But their relationship is nonlinear as shown in Fig. 6. The peak field intensity of a 2 MT TNT yield is 59 772 V/m and that of a 3 MT TNT equivalent energy is 76 171 V/m.

The figure shows that the slope of the curve decreases as the energy increases; the slope of curve when the energy is small is greater than that when the energy is great.

D. *Influence of Rising Time of the γ Rays*

In the foregoing calculations, every rising leading edge of γ ray is 7 ns, and the half width of the γ ray waveform is about 200 ns. But the calculations in the IEC standard (see Fig. 8) were conducted when the leading edge of γ ray is 2 ns, and the half width is about 15 ns. It is also noted that the total gamma ray yields for all calculations shown in this paper assume that each gamma ray yield is 0.1% of the total explosion yield. We selected the 2 ns leading edge γ time spectrum for another calculation and found that the rise time of HEMP is closely correlated to the rise time of γ rays, as shown in Fig. 9. The rise time of HEMP will not be faster than that of γ rays, but they are similar. The rise time presented in Fig. 7 is approximately 2.5 ns, with a half width of 10 ns.

E. *Transmission Laws of HEMP Above the Explosion Center*

To obtain HEMP parameters on satellite orbit, it is necessary to study the generation laws of HEMP in the upward transmission direction from the burst point. The calculation process was a bit different from that of downward transmission. It is necessary to introduce an earth-fixed coordinate system as

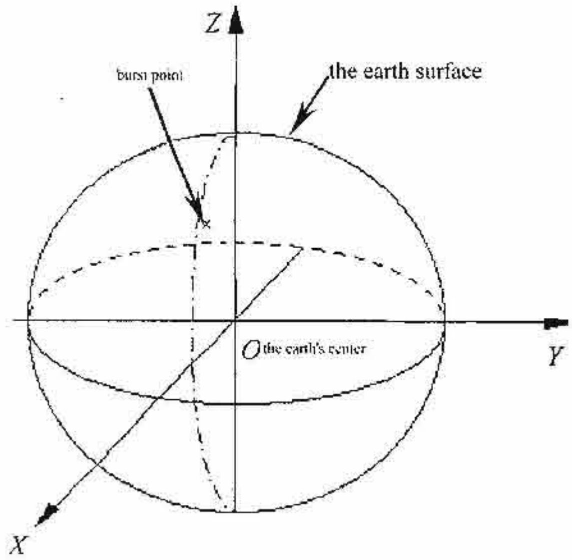

Fig. 9. Earth-fixed coordinate system.

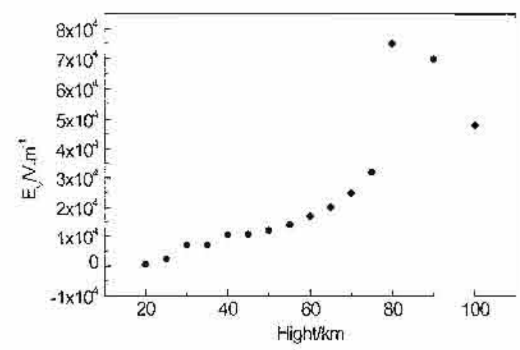

Fig. 10. Changes of the electric field intensity at different HOBs over the explosion center, with a 1 MT yield.

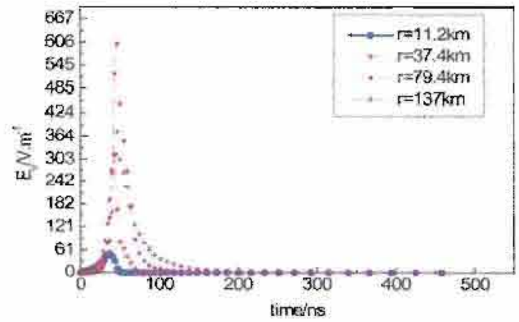

Fig. 11. Waveform of the electric field in the time domain, HOB is 20 km.

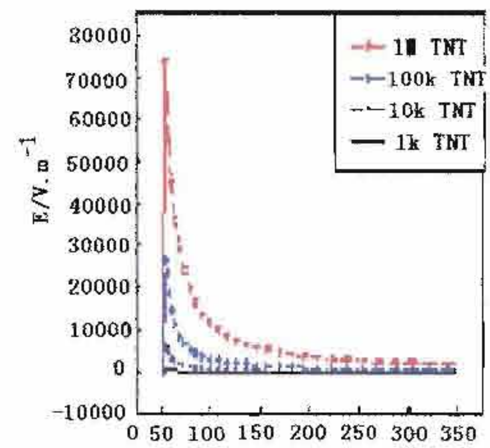

Fig. 12. HOB = 80 km, the waveform of electric field in the time domain at 150 km from the burst point.

opposed to the foregoing spherical coordinates. As the polar axis of spherical coordinates goes along the direction $\overline{B}_0$, and does not coincide with the vertical line of earth surface, there is no simple corresponding relation between the height (h) from the point of origin (r, θ, ψ) to the ground and the value of r. When waves are transmitted to the satellite orbit and when the satellite height is comparable to the earth's radius, the earth surface will not look like a flat surface. Then the position of any point on the satellite orbit in the spherical coordinate system cannot be expressed with a simple formula. The earth-fixed coordinate system is introduced (see Fig. 9) with its origin O at the earth's center, the flat surface XOY coinciding with the earth orbit surface. Axis OX coincides with the Greenwich meridian line. Axis OZ coincides with the polar axis of the earth. Thus, it will not be hard to find the position of points from the explosion center to a synchronous satellite orbit in the spherical coordinate system [13].

The calculation process was adjusted to provide the following result. Fig. 10 presents the curve of relation between the peak value of electric field and the height of explosion.

In addition, the calculation found that the electric field peak rises as the power increases. But their relationship is nonlinear too. Figs. 11 and 12 show the calculation results with different energies at explosion heights of 100 and 60 km. The power of the 100 kT explosion is 10 times less than that of the 1 MT nuclear explosion, with the electric field intensity peak down by 2.5 times; the power of 500 kT explosion is two times less than that of the 1 MT nuclear explosion, with the field intensity peak down by 15% only. As the power increases, the Compton-electron currents incited by the interaction of γ ray and air molecules grow, and the air conductivity increases too. Air conductivity is the damping term for electric field. They restrict each other to bring the electric field into the saturation area. Thus, the electric field intensity and energy will not change in a linear way.

Through calculations and analysis of the frequency range, with the effect of chromatic dispersion of the ionosphere considered, the low-frequency portion of source signals is reflected, and the high-frequency portion suffers chromatic dispersion by the ionosphere. Phases with high frequency have fast speed, those with low frequency have slow speed. The chromatically dispersed electric field becomes a damped oscillation waveform. In terms of the attenuation of amplitude, there is no change in the magnitude of peak values as compared with the former ones. The calculation resulted in the EMP field intensity at different explosion heights on the geosynchronous orbit when the total explosion energy is 1 MT (see Table II).

TABLE II
RELATIONSHIP BETWEEN THE ELECTRIC FIELD PEAK AND THE EXPLOSION HEIGHT FOR A SATELLITE ON GEOSYNCHRONOUS ORBIT (WITH YIELD OF 1 MT)

HOB (km)	Peak value of E-field, with distance of 150 km to the burst point (V/m)	Peak value of E-field, 36000 km Geosynchronous Orbit (V/m)
20	347.2	0.011
35	3926.0	0.114
40	4504.0	0.131
45	4764.5	0.138
50	4868.4	0.141
55	4835.0	0.140
60	4770.0	0.138
65	4512.5	0.130
70	4316.2	0.125
75	3966.6	0.115
80	3710.8	0.107
90	3000.0	0.087
100	2035.0	0.059

The numerical result is that after the 20–100 km nuclear explosion EMP is transmitted upward to the satellite orbit at 36 000 km, the field intensity peak of 1 MT TNT yield ranges from 10 to 100 mV/m; the field intensity peak of 1 kT yield ranges from 0.1 to 4 mV/m, and the background noise at this altitude is only 10 μV/m; therefore, HEMP signals could be detected. Thus, nuclear explosions above 1 kT can be detected theoretically. The effect of yield on EMP peak values is less severe than that for explosion height variations. Also the relationship between the field intensity with the yield and HOB is nonlinear.

V. CONCLUSION

Through calculations, it is easy to find that the time waveform of HEMP looks like a double exponential waveform. The rise time is closely correlated to the rise time of γ rays. The HEMP is fast when the γ ray output is fast; on the path of downward transmission of the HEMP from the burst point, the lower it goes, the narrower the half width of the waveform; at a point on the ground closer to the explosion center, the narrower the half width of the time waveform. The half width in the deposition region is $\sim$100 ns, while on the ground it is between 10 and 30 ns. Both in the deposition region and on the ground, the HEMP varies from 1000 to 80 000 V/m. With a fast rise time and a slow declining time, a HEMP waveform has abundant frequency spectra.

The numerical calculation result is that, after bursts between 20 and 100 km HOB, HEMP is transmitted upward to a satellite orbit at 36 000 km, and the peak value of electric field of 1 MT TNT yield ranges from 10 to 100 mV/m; the peak value of the electric field for a 1 kT TNT yield ranges from 0.1 to 4 mV/m, and the background noise there is only 10 μV/m; therefore, HEMP signals could be detected. Thus, a nuclear explosion above the magnitude of 1 kT can be detected theoretically. The effect of explosion yield on peak value is less severe than that of the explosion height. Also the relationship between the peak value of electric field with the power and explosion height are nonlinear.

ACKNOWLEDGMENT

The author acknowledges all the reviewers's suggestions. In particular, the author acknowledges Dr. Radasky, he modified the English of this paper and added technological explanation.

REFERENCES

[1] W. Radasky, "The effects of three high power EM threats on electric power threats," presented at the Euro. Electromagn., Toulouse, France, Jul. 2012.
[2] W. J. Karzas and R. Latter, "Satellite-based detection of the electromagnetic signal from low and intermediate altitude nuclear explosions," AD-616701, Jun. 1965.
[3] W. J. Karzas and R. Latter, "Detection of the electromagnetic radiation from nuclear explosions in space," *Phys. Rev.*, vol. 137, no. 5B, pp. 1369–1378, 1965.
[4] W. J. Karzas and R. Latter, "Electromagnetic radiation from a nuclear explosion in space," *Phys. Rev.*, vol. 126, no. 6, pp. 919–927, 1961.
[5] T. C. Chapman, "A computer code for high altitude EMP," AD-777841, Jan. 1974.
[6] T. Murphy, "Electromagnetic pulse (EMP) from surface burst," LA-11060-MS, Aug. 1987.
[7] J. R. Lillis, "Theory of the high altitude electromagnetic pulse," AD-67418, Mar. 1974.
[8] F. M. Tesche and P. R. Barnes, "Development of a new high altitude electromagnetic pulse (HEMP) environment and resulting overhead line responses," *IEEE Trans. EMC*, vol. 34, no. 6, pp. 93–99, May 1992.
[9] C. L. Longmire and R. M. Hamilton, "A nominal set of high-altitude EMP environments," ORNL/Sub-86-18417/1, Feb. 1988.
[10] C. Meng, "The numerical research of the effect of the transient electromagentic field coupled to the multiple hole object," *High Power Laser Particle Beams*, vol. 12, no. 06, pp. 732–736, 2000.
[11] C. Meng, "Numerical simulation of the early-time high altitude electromagnetic pulse," *Chin. Phys.*, vol. 12, no. 12, pp. 571–576, 2003.
[12] C. Meng, "Effects of the HOB and the burst yield on the properties of NEMP," *Chin. J. Comput. Phys.*, vol. 20, no. 2, pp. 173–176, 2003.
[13] C. Meng, "The analysis of the propagation of transient electromagnetic pulse through ionosphere," *Nuclear Electron. Detect. Technol.*, vol. 24, no. 4, pp. 369–374, 2004.
[14] *Electromagnetic Compatibility (EMC) - Part 2: Environment - Section 9: Description of HEMP Environment - Radiated disturbance*, IEC 61000-2-9 Ed. 1.0, Feb. 1996.
[15] C. L. Longmire, "On the electromagnetic pulse produced by nuclear explosions," *IEEE Trans. Electromagn. Compat.*, vol. 23, no. 6, pp. 1897–1902, 1976.
[16] K. D. Leuthauser, "A complete EMP environment generated by high-altitude nuclear bursts," Theoretical Note 363, Oct. 1992. Available: http://ace.unm.edu/summa/notes/TheoreticalPDFs/TN364.pdf

Cui Meng (M'08) received the bachelor degree from Fudan University, Shanghai, China, in 1992 and the Doctor degree from Northwest Institute of Nuclear Technology, China, in 2003.

She did Postdoctoral Research in Tsinghua University, Beijing, China, during 2005–2007, and became an associate professor of Department of Engineering Physics, Tsinghua University, in 2007. Her current research interests include numerical simulating of high power electromagneitc environment,measurement of high power transient EMP.